PROCEEDINGS OF THE CANADIAN SOCIETY FOR MECHANICAL ENGINEERING INTERNATIONAL CONGRESS 2023
CSME CONGRESS 2023
JUNE 5-8, 2023, SHERBROOKE, QC, CANADA

CONTROL OF A MODIFIED DOUBLE INVERTED PENDULUM USING MACHINE LEARNING BASED MODEL PREDICTIVE CONTROL

Amirreza Yasami[1*], Arezoo Vafamand[1], Alexander Jordan[1],Hoseinali Borhan[2]
Charles Robert Koch[1], Mahdi Shahbakhti[1] ,
[1]Department of Mechanical Engineering, University of Alberta, Edmonton, Canada
[2]Cummins Inc, Columbus, IN 47201, USA
[*]ayasami@ualberta.ca

***Abstract*—A Machine Learning based Controller (MLC) is developed for a Modified Double Inverted Pendulum on a Cart. First, the governing differential equations of the system using the Lagrangian method have been derived. Then, a dataset for training and testing the machine learning-based models of the plant is generated. Next, different types of machine learning models such as artificial neural networks (ANN), deep neural networks (DNN), long-short-term memory neural networks (LSTM), gated recurrent unit neural networks (GRU), and recurrent neural networks (RNN) are used to capture the dynamics of the system. DNN and LSTM are selected, because of their superior performance compared to the other models. Finally, different variations of the Model Predictive Controller (MPC) have been designed and their performance is evaluated in terms of running time, and tracking error. The advantage of the proposed control methods in comparison with the conventional nonlinear and linear model predictive control method is demonstrated in simulation.**

***Index Terms*—Double Inverted Pendulum, Nonlinear Model Predictive Control, Deep Neural Network.**

I. Introduction

An inverted pendulum is a standard platform for control engineers to test new control techniques since it is nonlinear, unstable, complex, and under-actuated. It can be used to represent a wide range of applications such as rockets, cranes, and robots. Different configurations of the inverted pendulum are found in the literature such as a rotational single-arm pendulum [1], a cart inverted pendulum [2], a double inverted pendulum [3], a double link rotatory inverted pendulum [4], and a triple inverted pendulum [5]. Control of a Modified Double Inverted Pendulum on a Cart(MDIPC) is considered in this paper. MDIPC control consists of these operating models: (1) Pendulum swing up and stabilization at an unstable position. (2) Moving the cart to a desired position while stabilizing the pendulum. (3) Tracking control of pendulums' angle and the cart position.

Neural Networks (NNs) for modeling and controlling complex systems [6] and Fuzzy Logic Controllers (FLCs) which are intelligent human-like control used to control a double inverted pendulum on a cart (DIPC) in [7]–[9]. One advantage of FLCs is that they are quite simple and when compared to a Linear Quadratic Regulator (LQR) the FLC performed better under a variety of initial conditions with reduced peak levels [7]. A robust adaptive fuzzy controller is designed to balance pendulums in the upright position [8]. To improve the performance of the controller the parameters which are associated with the membership functions and rules are optimized by using either Genetic Algorithm (GA) or NNs. However, the traditional type 1 fuzzy logic system has been found to have limitations in treating large uncertainty and unexpected disturbances [9]. Thus, a type 2 FLC to compensate for these limitations show that the FLC has better stability and uncertainty [9]. A PD-type Fuzzy Iterative Learning Control (ILC) is designed for a single arm planner on a cart [10]. A linear and a nonlinear model are obtained and then based on the fuzzy logic the parameters of PD-ILC are re-tuned. A disadvantage of FLC is that the number of rules increases exponentially with the increase of input variables [8].

Artificial Neural Network (ANN) is another method that is used for a DIPC [6], [11]. Data that does not cover the full range of motion is used in feedforward NN design [6], and NN control performance is much worse than LQR. A Wavelet Neural Network (WNN), which has the advantages of simple structure and fast convergence, is designed and the weights of the hidden layer are optimized by using an Improved Genetic Algorithm (IGA) and has a good performance [11]. Although FLC and NN have good performance, no guarantee of stability is available. The DIPC model is linearized, and adaptive state feedback is implemented [12]. The control gains are adapted based on sliding mode surface relations and Particle Swarm Optimization (PSO) [12]. Pole placement and LQR methods are used [13]. The model is first linearized about the pendulum's upright position and state and control weighting matrices of LQR are optimized by using GA and PSO in single objective optimization. The upright of the two pendulum links and commanding the cart to a new position is the objective. A

combination of PID and reinforcement learning is developed when Q learning is combined with PID compensation to improve the slow convergence rate of PID and guarantee good tracking performance [14]. A two-cascade linear MPC controller is designed for an inverted pendulum system when the inner control loop, stabilizes the pendulum's angle and the outer loop adjusts the inner controller input to stabilize the cart position [15]. The trajectory tracking problem for a two-wheeled inverted pendulum vehicle is considered [16]. To simplify the system and reduce the computation burden input-output feedback linearization is carried out before designing MPC. Control of the position of the cart and the angle of two pendulum links using a combination of the MPC method and Machine Learning algorithms (ML) is examined in this paper.

A Schematic of the MDIPC is shown in Fig.1. For accurate reference tracking using MPC, an accurate model is needed. The nonlinear properties of MDIPC mean that a linearized model is too simplified for MDIPC. A nonlinear physics-based model is used to represent the MDIPC. Thus, the model will be used to generate data" for the subsequent data-driven control method. A nonlinear ML-based model is developed for the system based on the physical model and embedded in the MPC. Reducing the computation cost and increasing the accuracy of the controller in comparison with the conventional nonlinear and linear MPC is the main goal of this study. Simulations are compared with the case where the governing nonlinear and linear equations of the system are used as the prediction model for the MPC.

The remainder of this paper is organized in sections. In Section II, a physical model of MDIPC is derived. In Section III, the physical model is used to generate data which is then used for modeling. Data-driven models developed from the generated data are described in Section IV. Finally, in Section V, MPC is designed for the models, while the concluding remarks are given in Section VI.

II. MDIPC Physical Model With Motion in Plane

A Modified Double Inverted Pendulum on a Cart (MDIPC) system has a cart and two links which are shown in Fig.1. The control inputs are a horizontal force to the cart and two torques at the pendulums' joints. Since the MDIPC is unstable, this complicates generating rich data and for data-driven modeling developing ML models is dependent on the data, and persistently exciting data is needed to identify the system. To simplify the system and allow suitable data, the DIPC system is modified by adding two torsional springs at each of the joints and a linear spring that connects the cart to a wall; with two joint torques, the system is stable, so abundant data can be generated for the training of ML models. The angle of the lower (θ_1) and upper pendulum (θ_2), and the cart's position (θ_0) are considered as the system's outputs and are shown in Fig.1. The force that will be applied to the cart (u) and the torque which will be applied to lower (t_l) and upper (t_u) joints are the inputs of the system. The governing differential equations of the system are derived

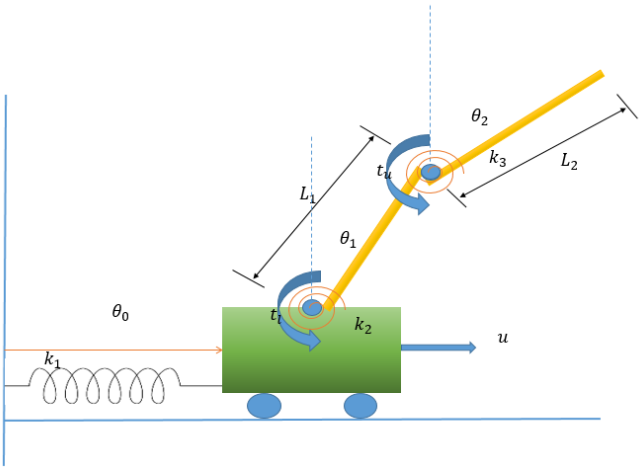

Fig. 1: Modified Double Inverted Pendulum on a Cart

using the Lagrange method by calculating the kinetic and potential energy of the system. The Lagrange equations are:

$$\frac{d}{dt}\left(\frac{\partial L}{\partial \dot{\theta}}\right) - \frac{\partial L}{\partial \theta} = q \tag{1}$$

where $\theta = [\theta_0, \theta_1, \theta_2]$ which are described above. In the Lagrangian L, q is defined as a vector of generalized forces that acts in the direction of each component in θ. The control force $u(t)$ is the force on the cart, and t_l and t_u are the torque of the lower and upper pendulum link, respectively. The Lagrangian is defined based on kinetic energy (E_{kin}) and potential energy (E_{pot}).

$$L = E_{kin} - E_{pot} \tag{2}$$

The position of the center of the mass of the cart is $x_0 = 0$, $y_0 = 0$, and the position of the center of the mass for the lower and upper pendulum links are.

$$\begin{aligned} x_1 &= \theta_0 + l_1 \sin(\theta_1)\,, y_1 = l_1 \cos(\theta_1) \\ x_2 &= \theta_0 + L_1 \sin(\theta_1) + l_2 \sin(\theta_2) \\ y_2 &= L_1 \cos(\theta_1) + l_2 \cos(\theta_2) \\ l_1 &= L_1/2, l_2 = L_2/2 \end{aligned} \tag{3}$$

The kinetic energy and potential energy of the cart are:

$$E_{kin}^{[0]} = \frac{1}{2} m_0 \dot{\theta}_0^2,\ E_{pot}^{[0]} = \frac{1}{2} k_1 \theta_0^2 \tag{4}$$

For the lower pendulum, the results are:

$$\begin{aligned} E_{kin}^{[1]} &= \frac{1}{2} I_1 \dot{\theta}_1^2 + \frac{1}{2} m_1 (\dot{\theta}_0 - l_1 \dot{\theta}_1 \cos(\theta_1))^2 + (l_1 \dot{\theta}_1 \sin(\theta_1))^2 \\ E_{pot}^{[1]} &= \frac{1}{2} m_1 g l_1 \sin\theta_1 + \frac{1}{2} k_2 \theta_1^2 \end{aligned} \tag{5}$$

For the upper pendulum, the kinetic and potential energy is:

$$\begin{aligned} E_{kin}^{[2]} &= \frac{1}{2} I_2 \dot{\theta}_2^2 + \frac{1}{2} m_2 ((\dot{\theta}_0 - L_1 \dot{\theta}_1 \cos(\theta_1) - l_2 \dot{\theta}_2 \cos(\theta_2))^2) \\ &+ (L_1 \dot{\theta}_1 \sin(\theta_1) + l_2 \dot{\theta}_2 \sin(\theta_2))^2 \\ E_{pot}^{[2]} &= m_2 g (L_1 \cos(\theta_1) + l_2 \cos(\theta_2)) + \frac{1}{2} k_3 \theta_2^2 \end{aligned} \tag{6}$$

$$D(\theta)\ddot{\theta} + C(\theta,\ \dot{\theta})\ \dot{\theta} + G(\theta) = HU$$

$$D(\theta) = \begin{pmatrix} m_0+m_1+m_2 & (m_1l_1+m_2L_1)\cos(\theta_1) & m_2l_2\cos(\theta_2) \\ (m_1l_1+m_2L_1)\cos(\theta_1) & m_1l_1^2+m_2L_1^2+l_1 & m_2L_1l_2\cos(\theta_1-\theta_2) \\ m_2l_2\cos(\theta_2) & m_2L_1l_2\cos(\theta_1-\theta_2) & m_2l_2^2+l_2 \end{pmatrix}, H = \begin{pmatrix} 1 & 0 & 0 \\ 0 & 1 & 0 \\ 0 & 0 & 1 \end{pmatrix}, U = \begin{pmatrix} u \\ t_l \\ t_u \end{pmatrix} \quad (7)$$

$$C(\theta,\dot{\theta}) = \begin{pmatrix} 0 & -(m_1l_1+m_2L_1)\sin(\theta_1)\dot{\theta}_1 & -m_2l_2\sin(\theta_2)\dot{\theta}_2 \\ 0 & 0 & m_2L_1l_2\sin(\theta_1-\theta_2)\dot{\theta}_2 \\ 0 & -m_2L_1l_2\sin(\theta_1-\theta_2)\dot{\theta}_1 & 0 \end{pmatrix}, G(\theta) = \begin{pmatrix} -k_0\theta_0 \\ -(m_1l_1+m_2L_1)g\sin\theta_1 - k_1\theta_1 \\ -m_2gl_2\sin\theta_2 - k_2\theta_2 \end{pmatrix}$$

The kinetic and potential energies of the components and Lagrange method the governing differential equations are:

The parameters of the system are listed in Table I. In order to obtain the linear model, the governing equations of motion for the system are numerically linearized about $\theta = [0, 0, 0]$ to form the state space model by calculating the Jacobian of the equations which results in:

$$A = \begin{pmatrix} 0 & 1 & 0 & 0 & 0 & 0 \\ -6.5 & 0 & -3 & 0 & 1.6 & 0 \\ 0 & 0 & 0 & 1 & 0 & 0 \\ -16.9 & 0 & -25.8 & 0 & 47.4 & 0 \\ 0 & 0 & 0 & 0 & 0 & 1 \\ 3.7 & 0 & 19.9 & 0 & -78 & 0 \end{pmatrix}, D = \begin{pmatrix} 0 \\ 0 \\ 0 \end{pmatrix}$$

$$B = \begin{pmatrix} 0 & 0 & 0 \\ 4.4 & 11.2 & -2.5 \\ 0 & 0 & 0 \\ 11.2 & 97.5 & -75 \\ 0 & 0 & 0 \\ -2.5 & -75 & 123.3 \end{pmatrix}, C = \begin{pmatrix} 1 & 0 & 0 & 0 & 0 & 0 \\ 0 & 0 & 1 & 0 & 0 & 0 \\ 0 & 0 & 0 & 0 & 1 & 0 \end{pmatrix} \quad (8)$$

TABLE I: Nominal values of MDIPC

Parameters	Description	Value
$m_0(kg)$	Mass of the cart	1.5
$m_1(kg)$	Mass of the lower pendulum	0.5
$m_2(kg)$	Mass of the upper pendulum	0.75
$L_1(m)$	Length of the lower pendulum	0.5
$L_2(m)$	Length of the upper pendulum	0.75
$l_1(m)$	Center of mass for lower pendulum	0.25
$l_2(m)$	Center of mass for upper pendulum	0.375
$g(m/s^2)$	The gravitational acceleration	9.81
$k_1(N/m)$	Spring constant of cart	1
$k_2(Nm/rad)$	Spring constant of lower pendulum	1
$k_3(Nm/rad)$	Spring constant of upper pendulum	1.5

III. Black Box Model

To identify a system using input-output data, the models of interest must be excited. Here, the proposed model of the MDIPC is used as the unknown plant. A Pseudo Random Binary Sequence (PRBS), amplitude 0.0125 (N.m) for torques, 0.0125 (N) for the force, with a sample time of 0.05 seconds, is used as the input to the plant model. The generated input for the force to the cart is plotted in Fig.2 where 13 seconds simulation is shown. The resulting outputs are depicted in Fig.3.

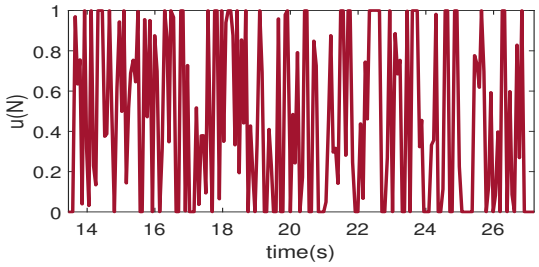

Fig. 2: MDIPC Input: Force for 13 seconds with PRBS input for model identification

IV. Data Driven Model Development

Based on the generated data, feed-forward and recurrent NN has been developed. The inputs of the model are the inputs of the system, including force and torques that are applied to MDIPC. This model will then be embedded in MPC since MPC performance depends on the quality of the model [17]. The model accuracy strongly influences the MPC performance. For training, validation, and testing $75\%, 10\%$, and 15% of the data are used. ANN and DNN have been developed for feed-forward networks and Recurrent NNs (RNN), Long Short-Term Memory (LSTM) and Gated Recurrent Unit (GRU) has been used for recurrent NN. To choose the hyper-parameters of the model, optimization is done to search systematically by using 'Ax' which uses the Sabol method to generate samples from a search space. The NN parameters that are chosen to be optimized are learning rate, dropout probability, number of hidden layers, type of activation function, and optimization method. The results are summerized in Table II.

DNN and LSTM have the best performance as seen in Table II where they have the smallest Mean Squared Error (MSE) and Mean Absolute Error (MAE), Root Mean Squared Error (RMSE), and correlation coefficient (R^2) and they estimate the system accurately. The DNN consists of 5 layers that each of which has 9 neurons with RELU activation function with a linear output layer's activation function. The LSTM consists of one hidden layer with 10 neurons with a $tanh$ activation

TABLE II: Nominal values of MDIPC

Model	DNN	LSTM	RNN	GRU
MSE	0.00	0.00	0.02	0.02
MAE	0.01	0.02	0.15	0.10
R^2	0.98	0.98	0.57	0.56
RMSE	0.01	0.03	0.12	0.13
RunTime(s)	89	108	208	284

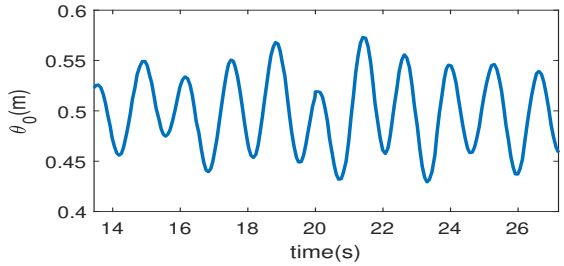

(a) Position of cart

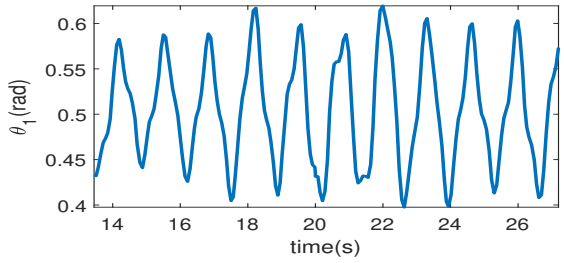

(b) Position of lower pendulum

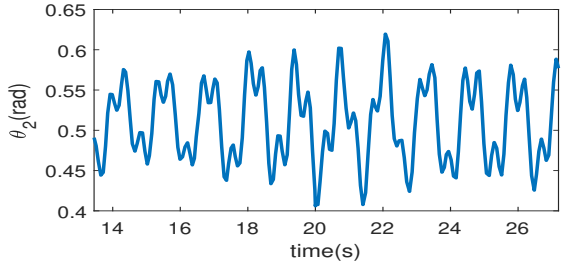

(c) Position of upper pendulum

Fig. 3: Output of the system for the generated input (Fig.2)

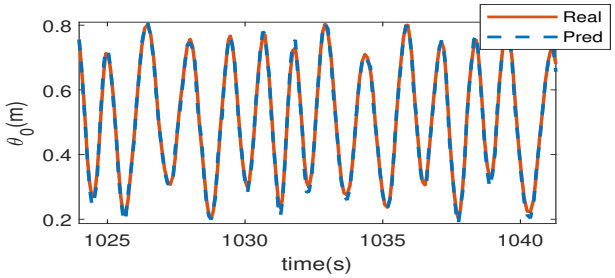

(a) Position of cart

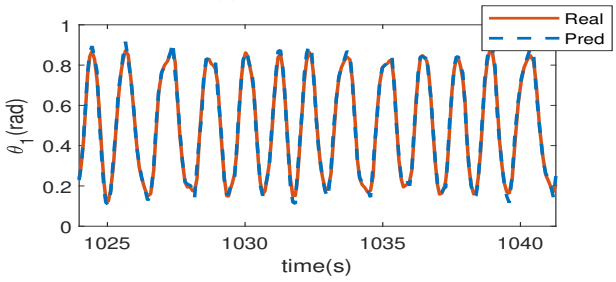

(b) Position of lower pendulum

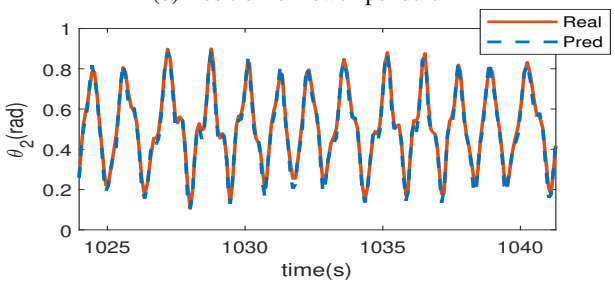

(c) Position of upper pendulum

Fig. 4: Comparing Real (red line) and Prediction (blue line) by using DNN

function, and the output layer is a dense layer with 3 neurons and a linear activation function. The test results for DNN are plotted in Fig.4 and Fig.5 for LSTM. For visual clarity in the plots, only a limited data range is depicted. As predictions in Fig.4 and Fig.5 show the results are accurate, and the developed models are acceptable.

V. Model Predictive Control Design

Now MPC is designed with the embedded based on one of DNN, LSTM, linear Eq (8), and nonlinear equations Eq (7). The block diagram of the plant and controllers is shown in Fig 6.

The performance of the ML-MPC controller is compared with the standard linear and nonlinear MPC. For nonlinear MPC, the 'NMPC' toolbox in MATLAB is used. The run times are on a desktop PC with a 12th Gen Intel(R) Core(TM) i7-12700K 3.60 GHz processor with 32.0 GB RAM. The NMPC cost function for obtaining the control law is a quadratic cost function;

$$J(N_p, N_u) = \sum_{j=1}^{N_p} \delta(j)[\hat{y}(t+j|t) - w(t+j)]^2 + \sum_{j=1}^{N_u} (\lambda(j)[\Delta u(t+j-1)]^2 + \mu(j)[u(t+j-1)]^2 + \rho(j)\epsilon^2) \tag{9}$$

where N_p is the prediction horizon, and N_u is the control horizon. The the general aim is that the future outputs on the considered horizon should follow a determined reference signal at the same time. Furthermore, the control rate Δu and control action can be considered in the cost function to reduce the jerk and the energy consumption, respectively. Also, the last term in the cost function is for the soft constraint.

The MDIPC has both hard physical constraints and soft constraints, which are constraints in the optimization. The hard constraints of this model consist of the position constraints or the cart position, and angle $[\theta_0, \theta_1, \theta_2]$ as well as the input force and torques applied $U = [u, t_l, t_u]$. The position of the cart θ_0 is bounded by the length of the track available here as ± 1. The angular positions $(\theta_1; \theta_2)$ are bounded between $\pm 180^\circ$ from the equilibrium position so that the system is

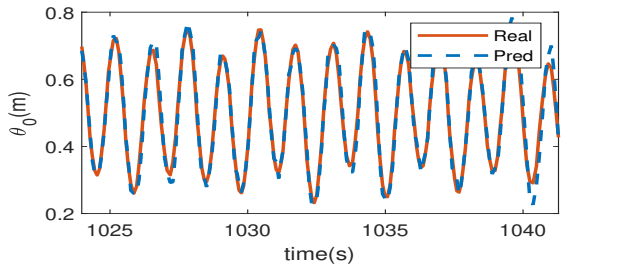

(a) Position of cart

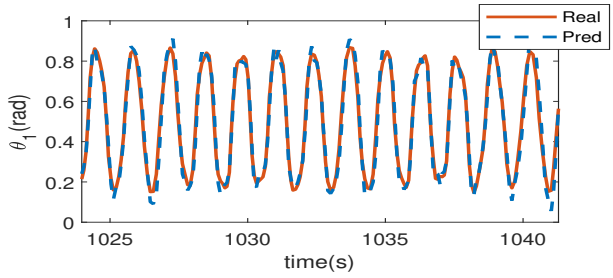

(b) Position of lower pendulum

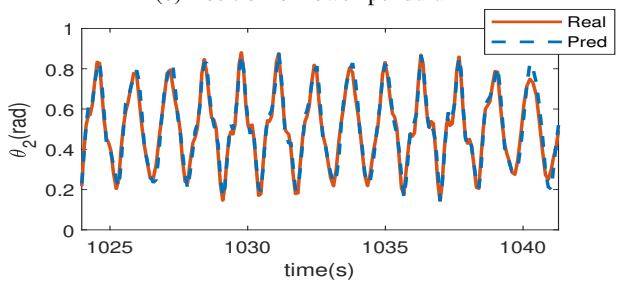

(c) Position of upper pendulum

Fig. 5: Comparing Real (red line) and Estimation (blue line) by using LSTM

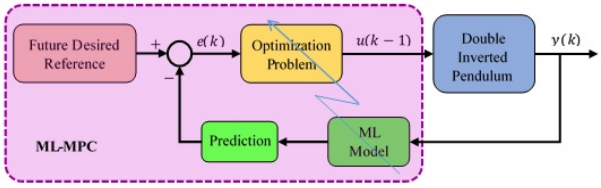

Fig. 6: Block diagram of ML and MPC

defined to not pass a full rotation. The manipulated variables $[u, t_l, t_u]$, are constrained based on the physical devices and limited to $\pm 0.0125N$ or $\pm 0.0125N.m$. Soft constraints on manipulated variables are introduced later in MPC design to further improve the performance of the controlled system. The parameters of the designed NMPC are listed in Table III. The results of ML-MPC, the linear and nonlinear MPC are plotted in Fig.7. For the linear MPC, the linear model of Eq(8) is used, and for the nonlinear MPC, the nonlinear model of Eq(3) is used. The results are then compared with ML-MPC with DNN and LSTM as the ML model. To demonstrate that the controller does not violate the constraint, they are plotted with a gray dashed line in Fig.7.

The linear MPC simulation has the worst performance and does not track the reference, and the control input is

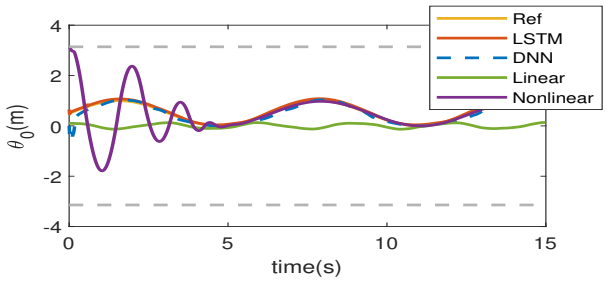

(a) Position of cart

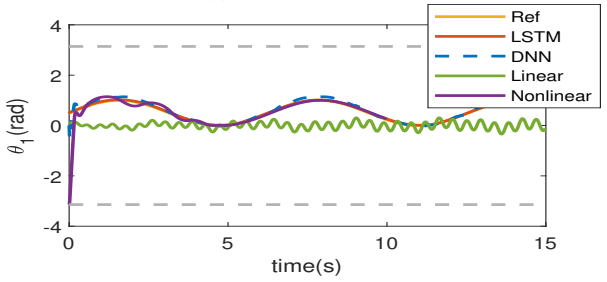

(b) Position of lower pendulum

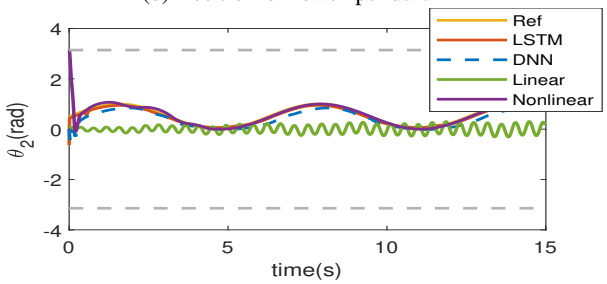

(c) Position of upper pendulum

Fig. 7: The outputs of the system for NMPC- DNN (blue line), LSTM (red line), ref (yellow line), and Linear (green dash line) with constraint (purple dash line)

continuously switching, resulting in poor tracking. The ML-MPC with DNN and LSTM have good tracking performance without violating the constraints. Comparing the results of ML-MPC with the nonlinear MPC shows that ML-MPC has better tracking performance and lower computation time. The control performance is summarized in Table IV. The DNN-MPC requires an order of magnitude less computation time than that of the ML-MPC combined with lower MSE and MAE.

VI. Conclusion

Nonlinear MPC where the embedded model is based on machine learning is developed for Modified Double Inverted Pendulum on a Cart. A physical model of the system is obtained and linearized. Then, the nonlinear model is used with PRBS inputs to develop a machine-learning model of the system to predict. DNN and LSTM ML models were developed, and the results show that ML-MPC has a better performance compared with the MPC physical models (linear, nonlinear). The simulation results demonstrated that the DNN-based nonlinear MPC offers the best performance among all

TABLE III: Parameters of designed MPC

Parameter	Linear-MPC	DNN-NMPC	LSTM-NMPC	Nonlinear-MPC
W-Output($\delta(j)$)	[10,10,10]	[13,14,15]	[1000, 1500,1000]	[100 100 100]
W-ContVariable($\mu(j)$)	[0.1,0.1,0.1]	[100,100,100]	[10,10,10]	[1 1 1]
W-ContVariableRate($\lambda(j)$)	Not considered	[1,1,1]	[0.1,0.1,0.1]	[0.1,0.1,0.1]
W-SoftConstraint$\rho(j)$	0.001	0.001	0.001	0.001
ContHorizon(N_u)	5	10	10	10
PredHorizon(N_2)	1	1	2	1

TABLE IV: Comparing Linear, DNN & LSTMC results

Metric	Output	Linear-MPC	DNN-NMPC	LSTM-NMPC	NonLinear-MPC
MSE	θ_0	0.37	0.0083	0.0438	0.1292
	θ_1	0.38	0.0076	3.4e-4	0.0177
	θ_2	0.37	0.0268	0.0031	0.0086
MAE	θ_0	0.50	0.0635	0.0025	0.0995
	θ_1	0.50	0.0668	0.0175	0.0342
	θ_2	0.50	0.0521	0.0506	0.0285
RunTime(s)		1.18	15.21	194.35	162.00

tested versions of MPC in terms of tracking and computational cost.

ACKNOWLEDGEMENTS

We would like to express our sincere gratitude to MahamadAli Tofigh, who served as our Teaching Assistant. His invaluable assistance and support throughout the semester helped us to understand the material more thoroughly and improve our skills.

REFERENCES

[1] M. F. Hamza, H. J. Yap, I. A. Choudhury, A. I. Isa, A. Y. Zimit, and T. Kumbasar, "Current development on using rotary inverted pendulum as a benchmark for testing linear and nonlinear control algorithms," *Mechanical Systems and Signal Processing*, vol. 116, pp. 347–369, 2019.

[2] L. Messikh, E.-H. Guechi, and S. Blažič, "Stabilization of the cart–inverted-pendulum system using state-feedback pole-independent MPC controllers," *Sensors*, vol. 22, no. 1, p. 243, 2021.

[3] O. Gonzalez and A. Rossiter, "Fast hybrid dual mode NMPC for a parallel double inverted pendulum with experimental validation," *IET Control Theory & Applications*, vol. 14, no. 16, pp. 2329–2338, 2020.

[4] Z. B. Hazem, M. J. Fotuhi, and Z. Bingül, "Development of a fuzzy-LQR and fuzzy-LQG stability control for a double link rotary inverted pendulum," *Journal of the Franklin Institute*, vol. 357, no. 15, pp. 10529–10556, 2020.

[5] A. Kawala-Sterniuk, Z. Slanina, and S. Ozana, "Implementation of smoothing filtering methods for the purpose of trajectory improvement of single and triple inverted pendulums," in *AETA 2019-Recent Advances in Electrical Engineering and Related Sciences: Theory and Application*, pp. 214–223, Springer, 2021.

[6] M. H. Arbo, P. A. Raijmakers, and V. M. Mladenov, "Applications of neural networks for control of a double inverted pendulum," in *12th Symposium on Neural Network Applications in Electrical Engineering (NEUREL)*, pp. 89–92, IEEE, 2014.

[7] G. S. Maraslidis, T. L. Kottas, M. G. Tsipouras, and G. F. Fragulis, "Design of a fuzzy logic controller for the double pendulum inverted on a cart," *Information*, vol. 13, no. 8, p. 379, 2022.

[8] V. Mohan, A. Rani, and V. Singh, "Robust adaptive fuzzy controller applied to double inverted pendulum," *Journal of Intelligent & Fuzzy Systems*, vol. 32, no. 5, pp. 3669–3687, 2017.

[9] Z. Sun, N. Wang, and Y. Bi, "Type-1/type-2 fuzzy logic systems optimization with RNA genetic algorithm for double inverted pendulum," *Applied Mathematical Modelling*, vol. 39, no. 1, pp. 70–85, 2015.

[10] A. Norouzi and C. R. Koch, "Robotic manipulator control using pd-type fuzzy iterative learning control," in *2019 IEEE Canadian Conference of Electrical and Computer Engineering (CCECE)*, pp. 1–6, 2019.

[11] Q.-k. Song and D.-w. Li, "The design and stability study of double inverted pendulum controller," in *2014 Seventh International Symposium on Computational Intelligence and Design*, vol. 1, pp. 403–406, IEEE, 2014.

[12] M. Mahmoodabadi and N. Nejadkourki, "Optimal adaptive state feedback control for a three degree-of-freedom series-type double inverted pendulum system by using particle swarm optimisation," *Australian Journal of Mechanical Engineering*, pp. 1–10, 2022.

[13] M. K. Habib and S. A. Ayankoso, "Modeling and control of a double inverted pendulum using LQR with parameter optimization through GA and PSO," in *2020 21st International Conference on Research and Education in Mechatronics (REM)*, pp. 1–6, IEEE, 2020.

[14] A. Zeynivand and H. Moodi, "Swing-up control of a double inverted pendulum by combination of Q-learning and PID algorithms," in *2022 8th International Conference on Control, Instrumentation and Automation (ICCIA)*, pp. 1–5, IEEE, 2022.

[15] L. Messikh, E. H. Guechi, and M. Benloucif, "Critically damped stabilization of inverted-pendulum systems using continuous-time cascade linear model predictive control," *Journal of the Franklin Institute*, vol. 354, no. 16, pp. 7241–7265, 2017.

[16] M. Yue, C. An, and J.-Z. Sun, "An efficient model predictive control for trajectory tracking of wheeled inverted pendulum vehicles with various physical constraints," *International Journal of Control, Automation and Systems*, vol. 16, no. 1, pp. 265–274, 2018.

[17] E. F. Camacho and C. B. Alba, *Model predictive control*. Springer science & business media, 2013.